

# Integer and fractional charge Lorentzian voltage pulses analyzed in the framework of photon-assisted shot noise

J. Dubois,<sup>1</sup> T. Jullien,<sup>1</sup> C. Grenier,<sup>2,3</sup> P. Degiovanni,<sup>2</sup> P. Roulleau,<sup>1</sup> and D. C. Glattli<sup>1</sup>

<sup>1</sup>CEA, SPEC, Nanoelectronics group, URA 2464, F-91191 Gif-Sur-Yvette, France

<sup>2</sup>Université de Lyon-Fédération de Physique André Marie Ampère, CNRS-Laboratoire de Physique de l'École Normale Supérieure de Lyon, 46 Allée d'Italie, 69364 Lyon Cedex 07, France

<sup>3</sup>Centre de Physique Théorique (CHPT), Ecole Polytechnique, 91128 Palaiseau Cedex, France

(Received 28 January 2013; published 1 August 2013)

We study the injection  $n$  of electrons in a quantum conductor using voltage pulses applied on a contact. We particularly consider the case of Lorentzian voltage pulses. When carrying integer charge, they are known to provide electronic states with a minimal number of excitations, while any other type of pulses are accompanied with a neutral cloud of electron and hole excitations. We focus on the low-frequency shot noise arising when the excitations are partitioned by a single scatterer. Using periodic pulses, the physics can be discussed in the framework of the photon-assisted shot noise. Pulses of arbitrary shape and arbitrary charge are shown to give a marked minimum in the noise when the charge is an integer. The energy-domain characterization of the charge pulse excitations is also given using the shot-noise spectroscopy which reveals the asymmetrical energy spectrum of Lorentzian pulses. Finally, time-domain information is obtained from Hong-Ou-Mandel-type noise correlations when two trains of pulses generated on opposite contacts collide on the scatterer. For integer Lorentzian, the noise versus the time delay between pulse trains is shown to give a measure of the electron wave-packet autocorrelation function. In order to make contact with recent experiments, all the calculations are made at zero and finite temperatures.

DOI: [10.1103/PhysRevB.88.085301](https://doi.org/10.1103/PhysRevB.88.085301)

PACS number(s): 73.23.-b, 73.50.Td, 42.50.Ar

This paper addresses the on-demand injection of a small finite number of electrons in a quantum conductor for applications in quantum information or in the study of the electron full counting statistics. We consider the  $n$ -electron source based on the application of periodic voltage pulses on the contact of a conductor.<sup>1,2</sup> The purity of the source, the spectroscopy, and the time extension of electron pulses are analyzed by calculating the shot noise resulting from electron scattering in the framework of the photon-assisted shot-noise theory.

Controlling few degrees of freedom makes quantum effects more accessible and opens the way to perform simple quantum information processing. During the last 30 years, most advances have been obtained in quantum optics with the manipulation of single photons emitted by atoms or semiconductor quantum dots, and in atomic physics with optical arrays of trapped cold atoms or ions. The successful manipulation of quantum states in condensed matter is more recent and has been done with superconducting circuits and semiconductor quantum dots. A different approach in condensed matter is the time-controlled injection of one to few undistinguishable electrons in a ballistic conductor. This opens the possibility to entangle several quasiparticles but also to probe the full counting statistics<sup>3</sup> (FCS) with a finite number of electrons<sup>4</sup> or to realize electron flying qubits.<sup>5-7</sup> For these applications, the source must be clean, i.e., not creating more excitations than the number of charges injected. Here, we follow the proposal by Levitov *et al.* in Refs. 1 and 2 where voltage pulses  $V(t)$  are applied to a contact. For a quantized action  $e \int_{-\infty}^{\infty} V(t) dt = nh$ ,  $n$  integer, and  $h$  the Planck constant,  $n$  charges are injected. As the current  $\tilde{I}(t)$  emitted by the contact toward the conductor is at all times equal to  $\tilde{I}(t) = \frac{e^2}{h} V(t)$ , this is equivalent to write  $\int_{-\infty}^{\infty} \tilde{I}(t) dt = ne$  [note that the current  $I(t)$  flowing through the conductor differs

from  $\tilde{I}(t) dt$  by a transmission factor]. On the experimental level, the approach is appealing as it does not require the implementation of a quantum dot nor the combination of tunnel barriers or of several quantum point contacts. For quantum bit applications, this improves the reliability as the delicate circuitry simplifies and reduces only to that necessary for quantum logic gate implementation. On the conceptual level, this apparently naive approach involves a nontrivial physics. In general, the injection of the  $n$  charges is accompanied by a neutral cloud of electrons and holes. The beautiful theoretical observation of Ref. 1 is that a Lorentzian voltage pulse carrying one electron provides a minimal excitation state free of neutral excitations. More generally, a superposition of  $n$  Lorentzian voltage pulses of arbitrary width and position in time but all carrying a unit charge of same sign remains a minimal excitation state.<sup>1,2</sup> These results have triggered several relevant theoretical contributions<sup>4,8-12</sup> in which the property and potential use of the Lorentzian voltage pulses are discussed. An experimental implementation has been demonstrated.<sup>13</sup> This paper aims at presenting a theoretical toolbox to characterize these clean excitations and therefore to interpret recent and forthcoming experiments performed with Lorentzian voltage pulses.

## I. BACKGROUND AND OVERVIEW

Here, we briefly review the past approaches of time-controlled charge injection in a conductor. Then, we will present a summary of physics discussed and of the results presented in this paper.

Up to now, the present approaches and realizations have considered only single-charge injection. Single-electron pumps based on the Coulomb blockade of tunneling have been

first realized using ordinary metallic systems.<sup>14,15</sup> They have potential application in quantum metrology but are not suitable for our purpose. First, the conductor is usually not ballistic. This prevents the use of electrons for flying qubits. Second, the electrons are sequentially injected. The lack of quantum coherence between electron tunneling events makes the injection of trains of few undistinguishable electrons impossible while this property is necessary for FCS studies. Another approach is based on itinerant quantum dots obtained using surface acoustic waves.<sup>16</sup> The transport of single to two electrons along a depleted electron channel<sup>17,18</sup> has been demonstrated. This approach may also have application in metrology. Because of the long coherence time of the spin, the injected electrons can be used for spin-based qubit operation and to carry the spin quantum information between distant dots.<sup>17,18</sup> However, the orbital part of the wave function is not enough well control for an application as flying qubits in a ballistic channel. Finally, we consider the on-demand injection single-electron source realized with a quantum dot whose last occupied energy level is suddenly risen above the Fermi energy of the leads. It has been realized using a quantum mesoscopic capacitor<sup>19</sup> operated in the nonlinear regime.<sup>20</sup> The source is energy resolved, exactly as frequency-resolved single-photon sources. It enables new types of quantum experiments where single electrons are injected at tunable energy above the Fermi energy. Time-controlled single-charge sources using this approach have been reported in Refs. 17, 18, 20, 21, and 67 and considered theoretically in Refs. 8 and 22–28. This single-electron source can not generate a coherent train of undistinguishable electrons. Injecting more than one electron requires a different approach such as the one proposed by Refs. 1 and 2 and discussed here. This source based on voltage pulses fulfills the condition for application in flying qubits and in full counting statistics.

Therefore, this paper explores the properties of the on-demand injection of few indistinguishable electrons using periodic voltage pulses at frequency  $\nu$  applied on a contact with a range of parameters relevant to experiments.<sup>13</sup> The conductor considered is a two-terminal ballistic one-dimensional conductor. In the middle of it is a localized scatterer characterized by a tunable transmission, for example, a quantum point contact (QPC). We assume that the transmission is energy independent. In quantum optics language, the scatterer can thus be viewed as an electron beam splitter. The transmission is assumed energy independent. As remarked in the pioneering works or Refs. 1, 2, and 45, the few-electron source can be analyzed using the low-frequency shot noise expected when the injected electrons pass through a beam splitter. Indeed, all excitations are partitioned irrespective to their charge, and the shot noise  $S_I$  counts the sum of electron  $N_e$  and hole  $N_h$  excitations while the dc current counts their difference  $n = N_e - N_h$ . As the source is periodic, a natural framework is provided by the photon-assisted shot noise (PASN) theory,<sup>29–33</sup> and the Floquet scattering theory<sup>34</sup> can be used to efficiently compute physical quantities. The PASN has been experimentally investigated in Refs. 35 and 36. In this paper, we will consider the difference between the noise  $S_I \propto (N_e + N_h)$  measured with the voltage pulse  $V(t) = V_{dc} + V_{ac}(t)$  minus the transport shot noise  $S_I^{tr} \propto n$  with only  $V_{dc} = \langle V(t) \rangle$  applied on the conductor.<sup>37–44</sup> The resulting

excess noise  $\Delta S_I$  is proportional to the excess particle number  $\Delta N_{eh} = N_e + N_h - n$ . The noise minimization ( $\Delta N_{eh} = 0$ ) at given current  $I = e\nu(N_e - N_h) = nev$  leads to  $N_h = N_e = 0$ . We will see that this minimization implies that the voltage pulse must be a sum of Lorentzian with quantized charge. It is important to understand that the shot noise is a tool to analyze the excitation content of the source and requires a transmission  $D < 1$ . As shown in the following, it is proportional to the binomial partitioning factor  $D(1 - D)$  where  $D$  is the transmission. A perfect wire  $D = 1$  gives no noise even for finite excitation content. The definition of  $\Delta N_{eh}$  provides the number of excitations and does not depend on transmission.

In this paper, we will concentrate on the calculation of the excess shot noise for different examples of pulse shape. Lorentzian shape pulses with  $n$  charges per period correspond to exactly  $n$  excitations.<sup>1,2</sup> Pulses of arbitrary shape are shown to contain more excitations<sup>10</sup> whose number is calculated for sine, square, and rectangular wave shapes. We also address the case of noninteger charge pulses which was shown in Refs. 1 and 45 to be the dynamical analog of the Anderson orthogonality catastrophe problem.<sup>46</sup> The Anderson physics manifests in a marked minimum of neutral excitations for integer charge per period as theoretically observed in Ref. 10. These results are known and revisited here in the framework of PASN. The last parts of the paper contain results providing an analysis of the excitations in the energy and time domains. We consider, respectively, the shot-noise spectroscopy and the Hong-Ou-Mandel shot-noise correlations for colliding trains of electron pulses on a beam splitter.

The paper is organized as follows. In Sec. II, we introduce the basic physics of the photon-assisted effects in a quantum conductor with a contact driven by a periodic voltage source in the Floquet scattering approach. We then consider the PASN and the competition between PASN and the transport shot noise (TSN) when both a dc bias and an ac voltage are applied. We also give the expression of the photon-assisted current.

In Sec. III, we address the comparison between several types of integer charge pulses: the square, the sine, the rectangular, and the Lorentzian. Using the PASN results of Sec. I, we calculate the number of electron-hole pair excitations via the excess noise. For comparison with experiments, the computation is done for both zero and finite temperatures. The hierarchy of charge pulses regarding noise production is compared with the hierarchy based on photocurrent production.

Section IV addresses the case of noninteger charge pulses. We show that for all type of pulses, the number of electron-hole pairs rises for noninteger charges, but is always minimal for integer charges.

Section V provides an energy-domain characterization of the charge pulses using shot-noise spectroscopy. We compute the PASN as a function of an arbitrary dc voltage bias which provides a direct measure of the photoabsorption probabilities.<sup>10,29,35,36,47</sup> In particular, the Lorentzian pulses show an asymmetric PASN versus dc bias characteristic of the absence of hole-type excitations, while sine and square waves lead to symmetric PASN.

Finally, Sec. VI gives a time-domain characterization of the pulses by looking at the shot noise generated by trains of electrons colliding on the scatterer, in close analogy with optical Hong-Ou-Mandel (HOM) experiments.<sup>60</sup>

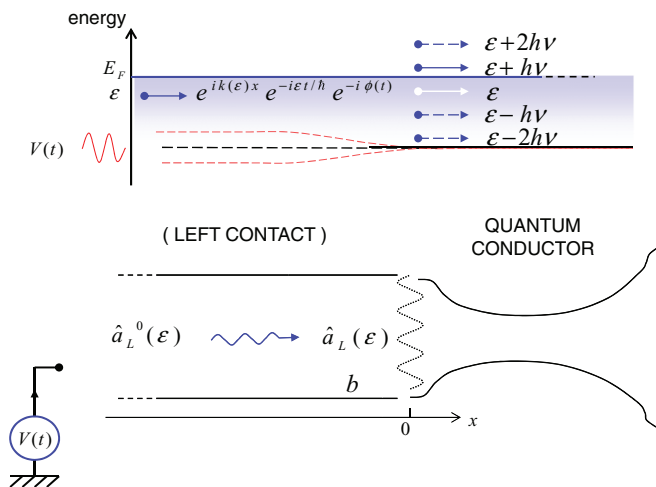


FIG. 1. (Color online) Under the effect of an ac voltage, electrons emitted far inside the contact acquire a time-dependent phase on their way to the scattering region (the quantum conductor). For periodic voltage, frequency  $\nu$ , the incoming electrons can be described by a quantum superposition of states at different energies  $\epsilon + lh\nu$ .

## II. FLOQUET SCATTERING DESCRIPTION OF PERIODIC VOLTAGE PULSES APPLIED ON A CONTACT

We consider a quantum conductor with one contact, say the left (L), periodically driven by a voltage  $V_{ac}(t)$  of frequency  $\nu = 1/T$  (see Fig. 1). Here, without loss of generality, we choose the approach of Refs. 30 and 48 where the periodic potential is assumed to be screened in all other regions of the quantum conductor. The voltage drop is assumed sharper than the electron wave-packet extension but smooth on the Fermi wavelength. The quantum conductor has a small width compared to that of the leads and a small length  $L$  compared with the electron phase coherence length  $l_\varphi$  such that electrons can propagate coherently over a length  $l_\varphi \gg L$  on the leads. Here,  $l_\varphi$  has to be estimated for the highest relevant energy of the problem, i.e.,  $\text{Max}(eV_{dc}, l_{\text{Max}}h\nu)$ , where  $l_{\text{Max}}h\nu$  is the largest relevant energy entering in a photon-assisted process. The region where electron loose coherence is called the reservoir or contact, following the standard description of the scattering theory of quantum transport. We assume that the electron transit time through the scattering region is short compared with the pulse width (and thus to the pulse period) such that energy-dependent phase terms can be neglected.<sup>33</sup> We consider an electron emitted by the left reservoir at energy  $\epsilon$  in a state  $\sim \exp[ik(\epsilon)x] \exp(-i\epsilon t/\hbar)$  with occupation probability  $f_L(\epsilon) = 1/[\exp(\epsilon/k_B T_e) + 1]$  where  $T_e$  is the electronic temperature and the Fermi energy is the zero-energy reference. From the left reservoir to the left entrance of the conductor, the electron experiences the potential  $V_{ac}(t)$  and its amplitude probability acquires an extra term  $\exp[-i\phi(t)]$ . The time-dependent phase is given by

$$\phi(t) = 2\pi \frac{e}{h} \int_{-\infty}^t V_{ac}(t') dt'. \quad (1)$$

The Fourier transform of

$$\exp[-i\phi(t)] = \sum_{l=-\infty}^{+\infty} p_l \exp(-i2\pi l\nu t) \quad (2)$$

gives the probability amplitude  $p_l$  for an electron to absorb ( $l > 0$ ) or emit ( $l < 0$ )  $l$  photons. Equation (2) expresses that an electron emitted at energy  $\epsilon$  enters the conductor in a superposition of quantum states at different energies  $\epsilon + lh\nu$ . The knowledge of the  $p_l$  completely defines the states of the incoming electrons. The magnitude of the  $p_l$  depends on the reduced quantity  $\alpha = eV_{ac}/h\nu$  where  $V_{ac}$  is the characteristic amplitude of the ac voltage. Combined with the scattering properties of the conductor, all photon-assisted effects resulting from the absorption or emission of energy quanta  $h\nu$  such as the ac current, the photocurrent or the photon-assisted shot noise can be calculated.

The properties of the  $p_l$  are best expressed in the framework of the Floquet scattering theory<sup>34</sup> in which the continuous energy variable describing states in the reservoir is sliced into energy windows of width  $h\nu$ , i.e.,  $\epsilon \rightarrow \epsilon + l'h\nu$  with  $\epsilon$  now restricted to  $[-h\nu, 0]$ . We can view the photon-assisted processes as the coherent scattering of electrons between the different energy windows. The scattering matrix  $S(\epsilon) = \{S_{ll'}\}$  relates the set of annihilation operators  $\hat{\mathbf{a}}_L^0(\epsilon) = \{\hat{a}_L^0(\epsilon + l'h\nu)\}$  operating on the states far inside the left contact to the set of annihilation operators  $\hat{\mathbf{a}}_L(\epsilon) = \{\hat{a}_L(\epsilon + lh\nu)\}$  acting on electronic states at the input of the conductor:

$$\hat{\mathbf{a}}_L(\epsilon) = S(\epsilon) \times \hat{\mathbf{a}}_L^0(\epsilon) \quad (3)$$

with  $\{S_{ll'}\} = p_{l-l'}$ . To satisfy the unitarity relations  $S^\dagger S = S S^\dagger = I$ , the amplitude probabilities show the useful relations

$$\sum_{l=-\infty}^{+\infty} p_l^* p_{l+k} = \delta_{k,0}. \quad (4)$$

In particular, the sum of the probabilities  $P_l = |p_l|^2$  to absorb or emit photons or to do nothing is equal to unity. As shown in Sec. IV, the probabilities  $P_l$  can be inferred from shot-noise spectroscopy, when in addition to the ac voltage a tunable dc voltage is applied between the contacts of the conductor. Note that the set of  $P_l$  does not contain all the information on the system. Indeed, the products  $p_l^* p_{l+k}$ ,  $k \neq 0$ , i.e., the nondiagonal part of the matrix density, enters in the calculation of the coherence<sup>47</sup> as discussed in Ref. 49.

### A. Photon-assisted shot noise

In the following, we compute the photon-assisted shot noise which occurs when the conductor elastically scatters the electrons. For simplicity, we will consider a single-mode (or one-dimensional) quantum conductor with transmission probability  $D$  as shown in Fig. 2.

Noise occurs only when an electron incoming from the left finds no incoming electron from the right or if a hole incoming from the left finds an incoming electron from the right. Indeed, because of the Pauli principle, or fermionic antibunching, the case where two electrons or two holes are simultaneously incoming gives no noise. In the former case, the incoming charges are randomly partitioned by the conductor with binomial statistics. At zero temperature and for zero ac voltage, the noise is zero. In the presence of an ac voltage, electron and hole excitations are created in the left lead. The photogenerated electrons span energies above the right-lead Fermi sea and the photogenerated holes below the

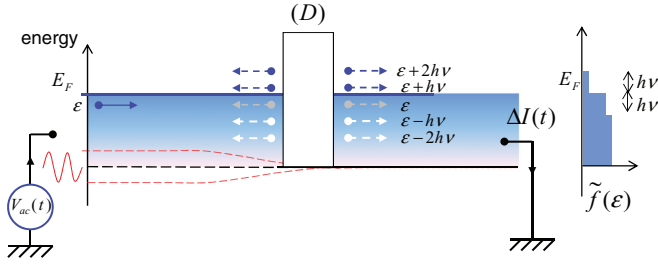


FIG. 2. (Color online) Electrons emitted by the left reservoir and pumped by the ac voltage in a superposition of states of different energy are scattered. The random partitioning between reflected and transmitted scattering states leads to current noise. The noise measures the sum of the number of holes and electrons which are photocreated. On the right is represented the energy distribution function  $\tilde{f}(\epsilon)$ . It should not be confused with an incoherent distribution function as the nondiagonal terms of the density matrix are nonzero.

right-lead Fermi sea. All the excitations contribute to partition noise, which is called the photon-assisted shot noise (PASN). According to Refs. 29 and 30, the low-frequency current noise spectral density due to photon-assisted process  $S_I^{\text{PASN}}$  is, including the Fermi distributions  $f_{L,R}(\epsilon)$  of the left and right reservoirs,

$$S_I^{\text{PASN}} = S_I^0 \int \frac{d\epsilon}{h\nu} \sum_{l=-\infty}^{+\infty} P_l \{ f_L(\epsilon - lh\nu) [1 - f_R(\epsilon)] + [1 - f_L(\epsilon - lh\nu)] f_R(\epsilon) \}, \quad (5)$$

where  $S_I^0 = 2 \frac{e^2}{h} D(1-D)h\nu$  is the typical scale of the PASN. The complete noise expression is obtained by adding the thermal noise of the reservoirs:  $4k_B T_e D^2 \frac{e^2}{h}$ . Its origin is the thermal fluctuation of the population in the reservoir and is not related to partitioning nor to photon-assisted processes. In absence of ac voltage,  $P_l = \delta_{l,0}$ , the full noise reduces to thermal noise  $4k_B T_e D \frac{e^2}{h}$  and vanishes at zero temperature, as discussed above.

In order to best extract the physics, we first consider the zero-temperature limit

$$S_I^{\text{PASN}} = S_I^0 \sum_{l=-\infty}^{+\infty} |l| P_l. \quad (6)$$

The sum in the right-hand side is directly proportional to the number of electrons and holes created, respectively, above and below the Fermi energy (chosen as the zero of energy). To understand this, let us consider for simplicity that only  $P_0$  and  $P_{\pm 1}$  are important and first concentrate on the absorption process. Electrons below the Fermi surface at energy  $\epsilon - kh\nu$ ,  $k$  positive integer, can be promoted to energy  $\epsilon - (k-1)h\nu$  with probability  $P_1$ . This global upward shift of the Fermi sea leaves the electron population unchanged below  $E_F$  but fills the empty states of energies  $\epsilon \in [0, h\nu]$  with occupation probability  $P_1$ , above  $E_F$ . Similarly, in the emission process, electrons are displaced to energies  $\epsilon - (k+1)h\nu$  with probability  $P_{-1}$ . The downward shift of the Fermi sea gives no net change of the population of states with energy  $< -h\nu$ , while for the energy range  $[-h\nu, 0]$  the population is now  $1 - P_{-1}$ . More generally, the  $l$ -photon processes give electron

excitations above the Fermi sea with population  $P_l$  in the energy range  $[0, lh\nu]$ ,  $l > 0$ , and hole excitations below the Fermi sea in the energy range  $[-lh\nu, 0]$  (see Fig. 2). As the current of electrons emitted by the left contact and able to create a  $l$ -photon electron excitation is  $(e/h)lh\nu = le\nu$ ,<sup>36</sup> the number of corresponding electrons created per period is  $lP_l$ . The total number of electron excitations generated per period is thus

$$N_e = \sum_{l=1}^{+\infty} l P_l \quad (7)$$

and similarly the number of holes

$$N_h = \sum_{l=-\infty}^{-1} (-l) P_l \quad (8)$$

and, from Eq. (6), the PASN is

$$S_I^{\text{PASN}} = S_I^0 (N_e + N_h). \quad (9)$$

To conclude this section, we must emphasize that the energy distribution function  $\tilde{f}_L(\epsilon) = \sum_{l=-\infty}^{+\infty} P_l f_L(\epsilon - lh\nu)$  depicted in Fig. 2 does not arise from a stationary state characterized by an incoherent nonequilibrium distribution. If this were the case, even for a perfect lead ( $D = 1$ ), one would expect a current noise associated with the population fluctuation  $\propto \int d\epsilon \tilde{f}_L(\epsilon) [1 - \tilde{f}_L(\epsilon)]$  as for thermal noise. In the present case, the terms  $p_l^* p_{l+k}$  contributing to the nondiagonal part of the density matrix should not be forgotten. For example, they are important for the multiparticle correlations considered by Moskalets *et al.*<sup>50</sup> or for the concept of electron coherence defined in analogy with quantum optics by Grenier *et al.*<sup>47,49</sup> These interference terms contribute to make the low-frequency photon-assisted shot noise *strikingly vanishing at unit transmission*. This was experimentally shown by Reydellet *et al.*<sup>36</sup> In this work, the theory of quantum partition noise of photon-created electron-hole pairs [Eqs. (6)–(9)] was experimentally checked from weak to large ac excitation and by varying the transmission. Motivated by this experiment, Rychkov *et al.*<sup>31</sup> have theoretically shown that the electron and hole excitations contributing to noise in Eq. (9) are not statistically independent. Equation (9) was derived by Lee *et al.*,<sup>51</sup> Levitov *et al.*,<sup>1</sup> and later by Keeling *et al.*<sup>2</sup> In the different context of periodic injection of energy-resolved single electron and single hole from a quantum dot, a similar equation has been derived and experimentally tested by Bocquillon *et al.*<sup>21</sup> for the partitioning of single charges, but  $N_e$  and  $N_h$  are not given by Eqs. (7) and (8) but originate from a different mechanism. Finally, as discussed in the following, it is important to note that Eq. (9) measures the number of electron and hole excitations accurately only at zero temperature.

### B. Photon-assisted and transport shot noise

We consider now a dc voltage bias  $V_{dc} > 0$  added to the periodic ac voltage  $V_{ac}(t)$  on the left contact while the right-lead Fermi energy remains zero. Let  $q = eV_{dc}/h\nu$  be the number of electrons emitted per period due to the dc bias. The total number of left electrons participating to noise is  $q + \sum_{l=1}^{+\infty} l P_l = q + N_e$ . The number of holes generating partition noise is, however, reduced by the positive shift of the

left Fermi energy. For  $(n-1)h\nu < q < nh\nu$  the number of holes participating to noise reduces to  $\sum_{l=-\infty}^{-n} (-l-q)P_l < N_h$ . The shot-noise expression (9) is then changed by replacing the  $|h\nu|$  terms by  $|h\nu + eV_{dc}|$  as originally derived by Lesovik *et al.* and later by Pedersen *et al.*<sup>29,30</sup> This result has been extended to the full counting statistics of electron transfer for PASN with dc bias by Vanevic *et al.*<sup>32</sup> In absence of ac voltage, one recovers the transport shot noise  $S_I^{\text{TSN}} = 2\frac{e^2}{h}D(1-D)|eV_{dc}|$ .

The mixed situation with both  $V_{ac}$  and  $V_{dc}$  leads to interesting effects due to the competition between PASN and TSN. They are best displayed using the excess noise where the pure TSN is subtracted from the total noise:

$$\Delta S_I = 2\frac{e^2}{h}D(1-D) \left[ \sum_{l=-\infty}^{+\infty} P_l |h\nu + eV_{dc}| - |eV_{dc}| \right]. \quad (10)$$

This would correspond to an experimental situation where the noise measured with  $V_{ac}$  on is subtracted from the dc transport shot noise measured with  $V_{ac}$  off while keeping the dc voltage on.<sup>10,13</sup>

Finally, we can write reduced units for the excess shot noise  $\Delta S_I = S_I^0 \Delta N_{eh}$ . Using the dc voltage in reduced unit  $q = eV_{dc}/h\nu$ , this gives

$$\Delta N_{eh} = \sum_{l=-\infty}^{+\infty} |l+q|P_l - |q|, \quad (11)$$

which represents at zero temperature the total number  $\Delta N_{eh}$  of photon-created electrons and holes not contributing to the TSN.

The derivative of the excess shot noise  $\Delta S_I$  (or of  $\Delta N_{eh}$ ) with respect to  $q$  shows remarkable singularities each time  $q = eV_{dc}/h\nu$  is an integer  $n$ . At the singularity, the change of slope of the variation of  $\Delta S_I$  with positive (negative)  $V_{dc}$  is proportional to  $2P_{-n}(2P_n)$  for  $n \neq 0$  and  $(2P_0 - 1)$  for  $n = 0$ . Varying  $V_{dc}$  thus provides direct information on the  $P_l$ . Their direct measure is provided by the second derivative of the noise:<sup>35,52,53</sup>

$$\partial^2 \Delta N_{e-h} / \partial q^2 = (2P_0 - 1)\delta_{q,0} + \sum_{l \neq 0} 2P_l \delta_{q,-l}. \quad (12)$$

Applying a monochromatic sine wave to a contact, the noise singularities at dc voltage multiple of the frequency has been observed in a diffusive metallic wire by Schoelkopf *et al.*<sup>35</sup> via the second derivative of the noise, giving the  $P_l$  spectroscopy. Later, the controlled suppression by a dc voltage bias of hole or electron excitation contribution to PASN has been discussed and observed in a quantum point contact by Reydellet *et al.*<sup>36</sup> The extracted set of  $P_l$  quantitatively agrees with the Bessel functions expected for the monochromatic sine wave used in the experiments<sup>35,36</sup> and considered in the first derivation of PASN,<sup>29,30</sup> as well in Ref. 32. Inferring the energy distribution of photon-excited electrons from shot-noise spectroscopy has been discussed in Ref. 52 and was compared to tunnel spectroscopy by Shytov.<sup>53</sup> In the different context of the energy-resolved single-electron and hole source using a mesoscopic capacitor, a similar shot-noise spectroscopy was proposed by Moskalets and Büttiker.<sup>8</sup> In this same context, the concept of shot-noise spectroscopy and

Eq. (12) has been extended to propose a full tomography of the electron and hole quantum states by Grenier *et al.*<sup>47</sup> The shot-noise spectroscopy is used in Sec. IV to analyze the excitation content of periodic charge voltage pulses.

Finally, directly relevant to the topics of charge injection, the singularity at  $eV_{dc} = nh\nu$  ( $q = n$ ) corresponds *exactly to the condition required for injecting  $n$  electrons per period.* This is why the presentation of periodic charge injection using voltage pulses is particularly relevant and enlightening in the framework of PASN. This singularity is also a useful tool to characterize the carrier charge in interacting systems. The superconducting-normal junction where conjugated electron-hole Andre'ev pairs carry twice the electron charge has been studied by Torres *et al.*<sup>54</sup> The finite-frequency PASN noise of charge  $e$  and charge  $e/3$  partitioned by a QPC was studied, respectively, in the integer and the fractional quantum Hall regime at  $\frac{1}{3}$  Landau level filling factor by Crépieux *et al.*<sup>55</sup> and later by Chevallier *et al.*<sup>56</sup>

For comparison with realistic experimental situation, we provide the excess noise formula at finite electron temperature  $T_e$ . We start from the expression of PASN derived at finite temperature by Lesovik and Levitov and by Pedersen and Büttiker<sup>29,30</sup> and rewrite it in reduced units to define the finite-temperature excess noise  $\Delta S_I(V_{ac}, V_{dc}, T_e) = S_I^0 \Delta N_{eh}(\alpha, q, \theta_e)$  where

$$\Delta N_{eh}(\alpha, q, \theta_e) = \sum_{l=-\infty}^{+\infty} (l+q) \coth\left(\frac{l+q}{2\theta_e}\right) P_l(\alpha) - q \coth\left(\frac{q}{2\theta_e}\right) \quad (13)$$

and  $\theta_e = k_B T_e / h\nu$  is the temperature in frequency units. At finite temperature,  $\Delta N_{eh}(\alpha, 0, \theta_e)$  no longer represents a direct measure of  $N_e + N_h$  as the excitations created in the energy range  $k_B T_e$  around the Fermi energy interfere with thermal excitations. This reduces the shot noise, which therefore misses these excitations.<sup>57</sup>

### C. Photon-assisted current

Finally, we consider another photon-assisted effect, the photocurrent, which also depends on the probabilities  $P_l$ . We consider a weakly energy-dependent transmission probability  $D(\varepsilon) \simeq D + \varepsilon \partial D / \partial \varepsilon$  and neglect the energy dependence of the transmission amplitude phase for simplicity. This situation is known to give a rectification effect characterized by a quadratic term in the low-frequency I-V characteristic of the conductor. In terms of photon-assisted effect, this leads to a dc photocurrent whose expression is

$$I_{ph} = \frac{e^2}{h} (h\nu)^2 \partial D / \partial \varepsilon \sum_{l=-\infty}^{+\infty} l^2 P_l. \quad (14)$$

One can see that  $I_{ph}$  gives information on the  $P_l$  and can discriminate between different types of ac signal. However, as shown in the next sections, it is not as useful as shot noise as it can not distinguish between electron and hole excitations and in particular can not identifies the minimal excitation Lorentzian pulses. Indeed,  $\sum_{l=-\infty}^{+\infty} l^2 P_l = \frac{1}{T} \int_0^T |d\varphi(t)/dt|^2 = (e/\hbar)^2 \langle V_{ac}(t)^2 \rangle$  and  $I_{ph}$  gives the same

information than a classical time averaging of  $V(t)^2$ . As the ac amplitude of the pulses  $V_{ac}$  is proportional to the average value  $V_{dc} = qh\nu/e$ , the photon-assisted current varies as the square of the injected charge as shown in Fig. 4. This quantity is also proportional to the production rate of heat in the contacts  $I(t)V(t) \propto V(t)^2$ .

### III. INTEGER PERIODIC CHARGE INJECTION

In this section, we give the expression of the probabilities  $P_l$  associated with various types of pulses carrying  $q = n$  charges per period: the sine, the square, and the Lorentzian. From the shot noise we establish the hierarchy of the pulses in terms of number of  $e$ - $h$  excitations  $\Delta N_{eh}$ . We also calculate the photocurrent and conclude that shot noise is the right quantity able to characterize the purity of the charge pulses. We consider a periodic excitation carrying a charge  $q = ne$  per period  $T = 1/\nu$ . This occurs if  $1/T \int_t^{t+T} V(t')dt' = nh\nu$ . It is convenient to decompose the voltage into its mean value  $V_{dc} = nh\nu$  and its ac part  $V_{ac}$ .<sup>10,13,32</sup>

For the sine wave  $V(t) = V_{ac}[1 - \cos(2\pi\nu t)]$ , we have  $V_{dc} = V_{ac} = nh\nu/e$ . The emission and absorption probabilities are given by integer Bessel functions with  $P_l = J_l(n)^2$  where  $P_l$  is calculated putting in the time-dependent phase only the  $V_{ac}$  term and not the dc voltage part. Then, we can directly use the PASN shot-noise formula with dc bias (11) to calculate the number of excitations ( $n > 0$ ). Similarly, for the square wave  $V(t) = 2V_{dc} = 2h\nu/e$  for  $t \in [0, T/2]$  and  $V(t) = 0$  for  $t \in [T/2, T]$  (mod  $T$ ). The probabilities are given by  $P_l = \frac{4}{\pi^2} \frac{n^2}{(l^2 - n^2)^2}$  for odd  $l - n$ ,  $P_l = 0$  for even  $l - n$ , and  $P_n(n) = \frac{1}{4}$ . Both the sine and the square wave have symmetric variation around zero voltage, which implies symmetric electron and hole excitation creation. With  $P_l = P_{-l}$ , Eq. (11) now writes

$$\Delta N_{eh} = 2 \sum_{l=n+1}^{+\infty} (l - n)P_l. \quad (15)$$

The above expression is useful to provide the asymptotic expression of  $\Delta N_{eh}$  at large  $n$  for square wave pulses:  $\Delta N_{eh}(n)^{sq} \simeq \frac{1}{\pi^2} [\ln(n) + \gamma + 2 \ln(2) - 1]$  where  $\gamma$  is the Euler constant. By contrast, the sine wave does not lead to a log divergence since  $P_l \simeq \frac{1}{2\pi l} (en/2l)^l$  for  $l \gg n$ . Figure 3 gives

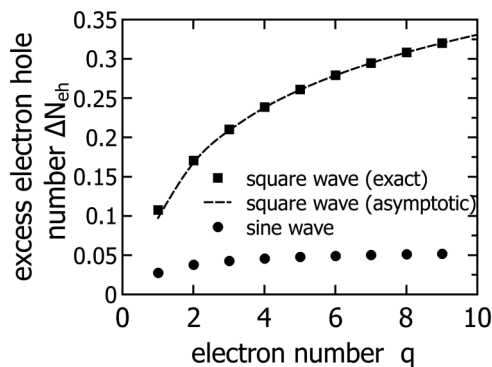


FIG. 3. Excess electron and hole particle number for sine and square wave pulses carrying  $q = n$  integer charges per period at zero temperature. The asymptotic log divergence of the square for large number, as defined in the main text, is shown as a dashed line.

$\Delta N_{eh}$  versus the number  $n$  of injected electrons for the square and the sine waves. Clearly, the square wave pulse creates more excitations than the sine wave.

We now consider the Lorentzian pulse whose behavior is quite different. As shown in the following, the  $P_l$  associated to the ac part of the voltage pulse remarkably vanishes for  $l < -n$ . The expression for the periodic sum of Lorentzian pulses where each pulse carries  $n$  electrons and the full width at half maximum (FWHM) is  $2W$  writes

$$V(t) = \frac{V_{ac}}{\pi} \sum_{k=-\infty}^{+\infty} \frac{1}{1 + (t - kT)^2/W^2}, \quad (16)$$

where  $eV_{ac} = nh\nu$ .

The total phase  $\Phi(t)$ , including the dc voltage part and using reduced time units  $u = t/T$  and  $\eta = W/T$ , gives

$$\exp[-i\Phi(t)] = \left( \frac{\sin[\pi(u + i\eta)]}{\sin[\pi(u - i\eta)]} \right)^n. \quad (17)$$

The above expression has only poles in the upper complex plane. This implies that its Fourier transform contains only positive frequencies. In physical terms, under total the application of Lorentzian voltage pulses, the electrons only absorb photons. This induces a global *upward shift of the Fermi sea* and no hole creation. Going back to the decomposition into dc and ac parts of the voltage

$$eV(t) = n \frac{h\nu}{2} \frac{\sinh(2\pi\eta)}{\sinh(\pi\eta)^2 + \sin(\pi u)^2} \quad (18)$$

with  $eV_{dc} = nh\nu$ , the amplitude probabilities associated with the only ac part are the Fourier transform of  $\exp\{-i[\Phi(t) - n\nu t]\}$  is

$$p_l = \int_0^1 du \left( \frac{\sin[\pi(u + i\eta)]}{\sin[\pi(u - i\eta)]} \right)^n \exp[i2\pi(l + n)u] \quad (19)$$

and the probabilities  $P_l = |p_l|^2$ . From the above consideration on the analyticity of  $\Phi$  we see that  $P_{(l < -n)} = 0$ . Note that this is consistent with vanishing negative frequency Fourier component for the total phase  $\Phi$  as the  $p_l$  differs from them by of shift of  $l$  into  $l - n$ .

For  $n = 1$ , we find  $P_l = 0$  for  $l < -1$ ,  $P_{-1} = \exp(-4\pi\eta)$ , and  $P_l = \exp(-l4\pi\eta)[1 - \exp(-4\pi\eta)]^2$  (see also Ref. 32). The expression of the  $P_l$  for integer charge number  $> 1$  involves the same exponential factor  $\exp(-l4\pi\eta)$  and a Laguerre polynomial. The complete expression is given in the next part as a special case of fractional charges  $q$  when  $q = n$ . Using  $\sum_{l=-n}^{\infty} lP_l = 0$  and Eq. (11) gives

$$\Delta N_{eh} = 0. \quad (20)$$

The excess shot noise vanishes and only the transport shot noise of  $n$  electrons remains. The Lorentzian pulses are therefore *minimal excitation states* as *no excess electron and hole excitations are created*. The  $n$  electronic excitations are, however, not concentrated on the energy window  $[E_F, E_F + eV_{dc}]$  but they occupy states above the Fermi energy with a weight exponentially decaying on the scale  $\sim \hbar/2W$ .

We also compare the photocurrent for different types of pulses (see Fig. 4). For the square and the sine waves with  $n$  electrons, the sum  $\sum_{l=-\infty}^{+\infty} l^2 P_l$  is 1 and  $\frac{1}{2}$ , respectively. This is consistent with the hierarchy found using shot noise which

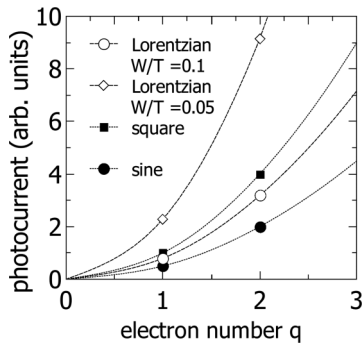


FIG. 4. Photocurrent in arbitrary units versus charge per period. We see that this photon-assisted effect can not probe the hierarchy of excitation content of different types of pulses. The dashed and dotted curves are guides for the eyes.

showed that the square contains more energetic excitations. For the Lorentzian, the sum is however nonzero and given by  $\coth(2\pi\eta) - 1$ . It strongly increases with the sharpness of the Lorentzian shape. We conclude that the photocurrent can not characterize the neutral excitation content of charge pulses.

IV. PERIODIC INJECTION OF ARBITRARY CHARGES

In this section, we calculate  $\Delta N_{eh}$  for arbitrary charge  $q$  carried per period. As in the previous section, we consider the square, sine, and Lorentzian pulse shapes and also include rectangular pulses. We show that  $\Delta N_{eh}$  oscillates with  $q$  and is locally minimal for integer  $q = n$ . For the sine wave  $P_l = J_l(q)^2$ , while for the Lorentzian case the calculation of the  $P_l$  for noninteger charges is less trivial. Physically, one may expect that carrying noninteger charges will involve more complex excitations. Mathematically, we immediately see that the term in the right-hand side of Eq. (17) is no longer analytic in the lower plane when  $q$ , replacing  $n$ , is not an integer. We thus expect a proliferation of hole excitations contrasting with the integer case. The calculation is done in the Appendix.

Figure 5 shows the  $P_l$  for periodic Lorentzian pulses of width  $W/T = 0.1$ . The absence of components for  $l \leq 1$  when

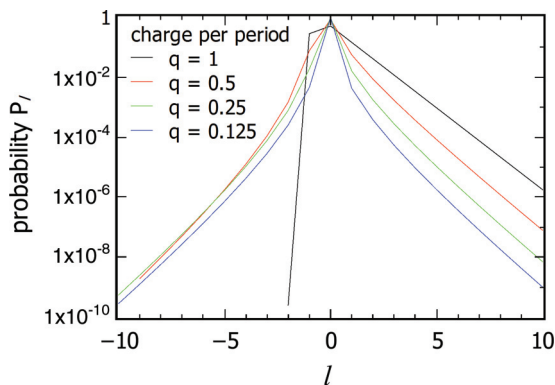


FIG. 5. (Color online) Absorption  $l > 0$  and emission  $l < 0$  probabilities corresponding, respectively, to electron and hole particle creation for periodic Lorentzian pulses of width  $W/T = 0.1$  and various charge  $q$  per pulse. The asymmetric spectrum for  $q = 0.99$  reflecting the lack of hole creation quickly leads to a symmetric spectrum for  $q \ll 1$ . Lines connecting the discrete  $P_l$  values are guides for the eyes.

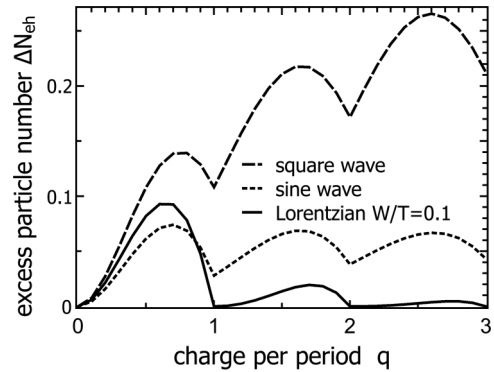


FIG. 6. Excess electron and hole particle for square, sine, and Lorentzian pulses carrying  $q$  charges per period. For the Lorentzian, the ratio  $W/T = 0.1$ .

$q = 0.99 \simeq 1$  strikingly contrasts with the case of  $q < 1$ . For small  $q$ , the  $P_l$  spectrum is almost symmetrical with  $l$  signaling nearly equal electron and hole pair excitation creation. Figure 6 shows the evolution of the excess particle number (or excess noise) versus  $q$  from 0 to 3 for square and sine wave pulses and for Lorentzian pulses of width  $\eta = W/T = 0.1$ . We observe that, even if the square and the sine do not provide minimal excitation states, they do provide a minimum of excitations for integer charges. This seems to be a remarkable property of the Fermi sea. A similar figure can be found in Ref. 10.

Figure 7, left, shows how the excess particle number evolves for Lorentzian pulses of different width. We see that for  $W/T \geq 0.1$  the particle number becomes exponentially weak. Indeed, the potential becomes close to a constant voltage  $V(t) \simeq V_{dc}$ . For small width and half-integer charge, the electron hole excitation number is large but quickly decreases with  $q$ , which contrasts with the almost constant value found for the sine wave and the increasing value for the square wave. For comparison, the right graph of Fig. 7 shows the excess particle content of discrete Dirac pulses (or rectangular pulses) of similar width  $W$  (the voltage pulses have amplitude  $h/eW$  for the time duration  $W$  and zero otherwise). Here again the excitation content is much larger. It increases with  $q$ , which contrasts with the Lorentzian pulse behavior which definitely shows the lowest noise.

It is interesting to see how the temperature affects the excess noise. As mentioned previously,  $\Delta N_{eh}$  no longer measures the number of excess electron and hole quasiparticles with good

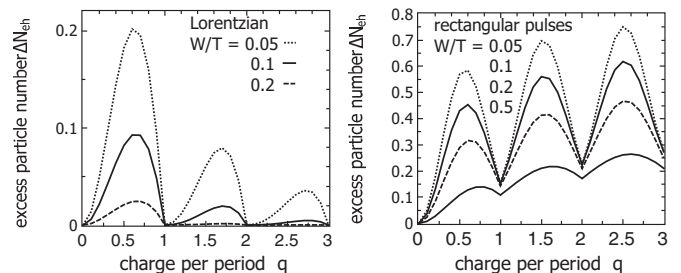


FIG. 7. Excess electron and hole particle number for Lorentzian (left) and rectangular (right) pulses carrying  $q$  charge per period and for different width to period ratio  $W/T$ .

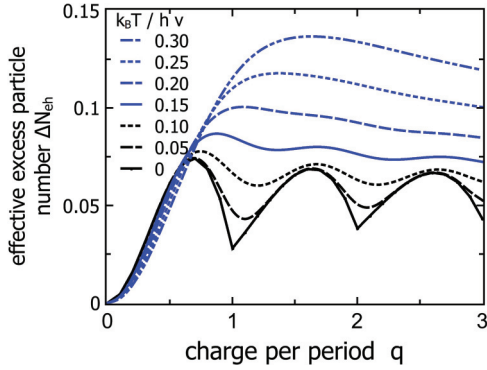


FIG. 8. (Color online) Effective excess electron and hole particle for sine pulses carrying  $q$  charges per period and for different values of the electron temperature  $T_e$ .

fidelity. For simplicity, we will keep the same notation but call it now the effective excess particle number. For sine and square waves, there is only one energy scale to compare with the temperature, i.e.,  $h\nu$ . For the Lorentzian case, there are two energy scales  $h\nu$  and  $\hbar/2W$ . Figure 8 shows the sine wave case. We observe that the minima occur to higher- $q$  values. The effect is even more pronounced for the case of Lorentzian voltage pulses shown in Fig. 9 and is probably related to the stronger asymmetry of  $\Delta N_{eh}$  with  $q$  around  $q = n$  for  $\eta = W/T = 0.1$ . This has been observed by Dubois<sup>13</sup> for sine and Lorentzian pulses and for the PASN shot noise of a biharmonic excitation by Gabelli.<sup>58</sup> The oscillations of  $\Delta N_{eh}$  are quickly damped by the temperature and when  $k_B T_e > 0.2h\nu$  are almost unobservable.

To end this section, it is worth to note that the noninteger charge considered here is injected in a noninteracting fermionic system (more precisely, a good Fermi liquid where interaction gives rise to Landau quasiparticles). Extension to fractional charges in Luttinger liquids has been considered by Ref. 2. The  $e/3$  fractional charge of fractional quantum Hall edge states has been considered by Jonckheere *et al.*<sup>59</sup>

### V. ENERGY DOMAIN: SPECTROSCOPY OF THE $e$ - $h$ PAIR EXCITATIONS

In this section, we use the shot-noise spectroscopy tool discussed in Sec. II to analyze the periodic charged states in

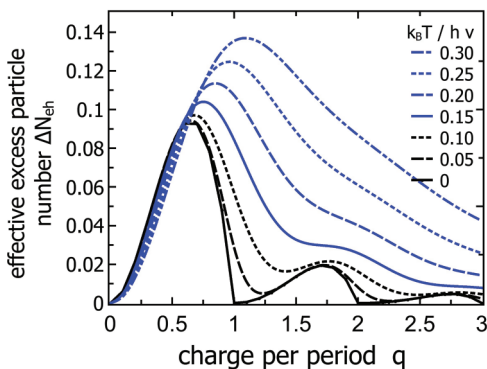


FIG. 9. (Color online) Effective excess electron and hole particle for Lorentzian pulses of width  $W/T = 0.1$  carrying  $q$  charges per period and for different electron temperature  $T_e$ .

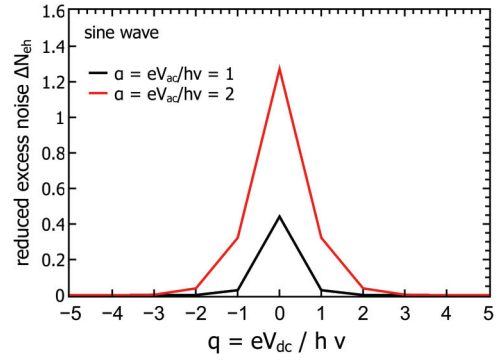


FIG. 10. (Color online) Zero-temperature excess partition noise versus dc voltage in reduced units for sine amplitudes  $\alpha = 1$  and 2 corresponding to single- and double-charge pulses when, respectively,  $q = 1, 2$ .

the energy domain. To do this, we compute  $\Delta N_{e-h}$  as a function of  $V_{dc}$ . Here, the dc bias  $q = eV_{dc}/h\nu$  is no longer linked to the ac amplitude parameter  $\alpha = eV_{ac}/h\nu$ . As explained in Sec. I, this allows us to make a spectroscopy of the electron and hole excitations and infer the  $P_l$  from the excess noise variation with  $V_{dc}$  or from the first or second noise derivative with respect to  $V_{dc}$ . The calculations and graphs are done and displayed at zero and finite temperatures.

Figures 10 and 11 show the variations of  $\Delta N_{e-h}$  versus  $q$  at zero temperature for, respectively, a sine wave and a Lorentzian wave. For each case, we show the curves for two different amplitudes  $V_{ac}$  corresponding to  $\alpha = 1$  and 2. These amplitudes would correspond, respectively, to single- and double-charge voltage pulses when  $q = \alpha = 1$  or 2, respectively. For sine and square waves  $\Delta N_{eh}(\alpha, q)$  is symmetric with  $q$  (or  $V_{dc}$ ) as  $P_l = P_{-l}$ . However, it is asymmetric for the case of Lorentzian pulses. Such asymmetry is expected for pulses whose ac part of the voltage is not symmetrical with respect to zero voltage. But, more relevant and striking, for the Lorentzian case the excess noise is zero for  $q > \alpha$  (or  $eV_{dc} > nh\nu$ ), a direct consequence of zero  $P_l$  for  $l < -n$ .

The effect of finite temperature is shown on Fig. 12 for a sine wave of amplitude  $\alpha = 1$ . Finite-temperature calculations are also shown in Figs. 13 and 14 for Lorentzian pulses of width

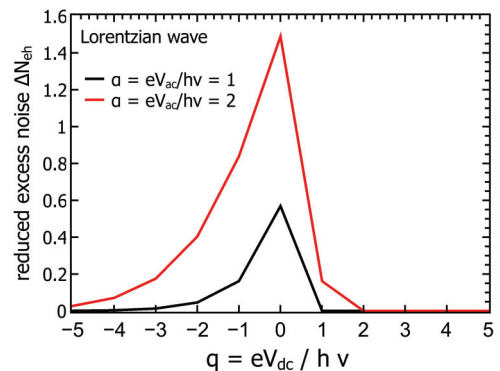


FIG. 11. (Color online) Zero-temperature excess partition noise versus dc voltage in reduced units for Lorentzian amplitudes  $\alpha = 1$  and 2 corresponding to single- and double-charge pulses when, respectively,  $q = 1, 2$ .



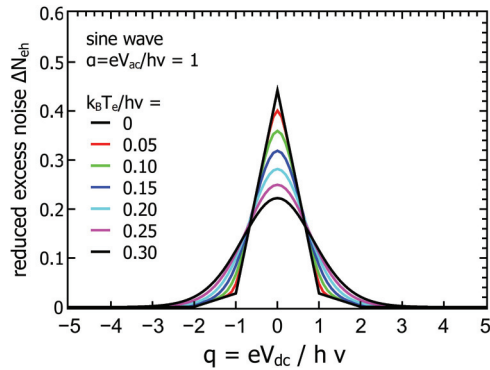


FIG. 12. (Color online) Finite-temperature excess electron and hole particle noise versus dc voltage in reduced units for sine wave of amplitudes  $\alpha = 1$ .

$W/T = 0.1$  with, respectively,  $\alpha = 1$  and  $2$ . The relevant temperature needed to reveal the asymmetry of  $\Delta N_{eh}$  with dc bias for a Lorentzian is given by the width, the smaller the width, the higher the energy  $\hbar/W$  at which we find the contributions of the positive  $P_i$  responsible for the long tail at negative voltages. The other temperature scale is given by the ratio  $k_B T/hv$  which controls the smoothing of the singularities at integer  $q$ .

**VI. TIME DOMAIN: SHOT-NOISE CHARACTERIZATION USING COLLISION OF PERIODIC CHARGE PULSES**

The time periodicity imposes that only information on a discrete energy spectrum is available and full characterization must be completed with a dual-time-domain information within a period. Here again, shot noise is the useful tool to provide this information. Inspired by the optical Hong-Ou-Mandel (HOM) correlation experiment, an electronic HOM analog can be built as a useful tool to infer the time shape of wave packets where electrons emitted from two contacts with a relative time delay collide on the scatterer. A clear relation between shot noise and wave-packet overlap can be made for a single-charge Lorentzian pulse. For other pulse shapes, it is expected that the contribution of the neutral excitation cloud gives an extra contribution to the shot noise.

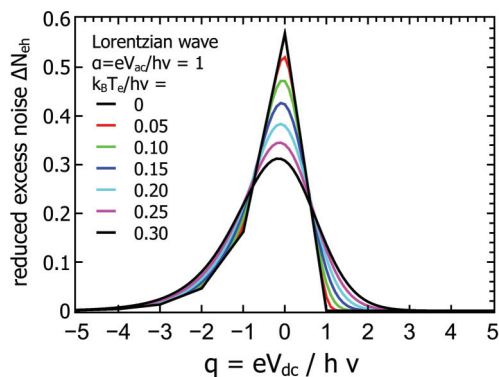


FIG. 13. (Color online) Finite-temperature excess electron and hole particle noise versus dc voltage in reduced units for Lorentzian waves of amplitude  $\alpha = 1$ .

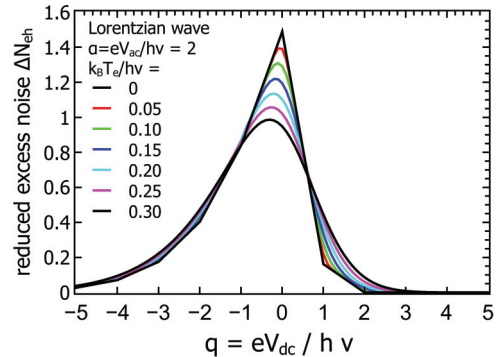


FIG. 14. (Color online) Finite-temperature excess electron and hole particle noise versus dc voltage in reduced units for Lorentzian waves of amplitude  $\alpha = 2$ .

In an optical experiment, single photons are emitted from two distinct sources in each of the two input channels of a semitransparent beam splitter. Photon detectors are placed on the two respective outputs and a time delay between them, sizable with the photon wave packet, is introduced. For zero delay, Bose statistics implies a constructive two-particle interference where the two photons bunch and exit, at random, in one of the two output channels. The coincidence events are zero and the particle fluctuations (the noise) are doubled with respect to a Hanbury Brown–Twiss (HBT) experiment where only one photon at a time arrives on the beam splitter. The latter situation is recovered when the delay  $\tau$  is much longer than the size of the wave packets. For intermediate time delays, the noise variation is directly related to the overlap of photon wave packets.<sup>60,61</sup> A similar experiment could be done with electrons with an artificial scatterer in the form of a controllable beam splitter, i.e., a quantum point contact. For zero time delay, Fermi statistics leads to a destructive interference for the probability of finding two electrons in the same output channel. In terms of charges counted by the detector (here the contacts of a conductor), there is always a charge arriving in each contact and consequently no current fluctuations. The noise increases from zero at  $\tau = 0$  to the single-particle noise value (similar to the photon HBT case) for time delay larger than the electron wave packet. The difference between fermion and boson for HOM correlations has been discussed by Loudon.<sup>62</sup> An electronic HOM experiment has been proposed by Giovannetti *et al.*<sup>63</sup> HOM shot-noise correlation of electron-hole pairs using two phase-shifted ac voltages of weak amplitude ( $eV_{ac} < h\nu$ ) has been theoretically considered by Rychkov *et al.*<sup>31</sup> Up to now, the theoretical works have only addressed the case not discussed here of two single charges emitted from two ac driven quantum dot capacitors. In this case, the HOM noise has been calculated by Ol’khovskaya *et al.*<sup>23</sup> In the adiabatic regime, the wave packets mimic those emitted by a contact driven by Lorentzian voltage pulses carrying a single electron followed by a single hole (note that, except for well-separated electron and holes, the alternate charge prevents to have clean excitations<sup>1</sup>). More recently, considering the same system, Jonckheere *et al.*<sup>28</sup> have looked to similar HOM correlations and include the effect of electron and hole collisions. Their analysis used the quantum electron optics framework developed by Grenier

*et al.*<sup>47,49</sup> Other recent theoretical works discussed various related situations.<sup>8,24,25,64</sup> In particular, Ref. 8 considered a mixed situation where electrons emitted from a quantum dot capacitor collide with electrons from a voltage pulse source. Here, we consider only voltage pulse electron sources. This regime was also addressed by Grenier.<sup>47</sup>

Practically, two generic situations, different in their geometry, provide similar information: the zero magnetic field case for which the reflected path physically coincides with the input path (this corresponds in optics to the mirror facing the two sources and detectors); the high magnetic field case, using the edge states of the quantum Hall regime where chiral propagation allows us to geometrically separate input and output channels. The first case provides simpler interpretation as the interaction is well screened [for example, the electrons reservoirs formed by a two-dimensional electron gas (2DEG) is a good Fermi liquid]. The second case better mimics the optical geometry, but the Coulomb interaction between copropagating quantum Hall edge channels leads to fractionalization of the injected pulses (see Ref. 49). Experimentally, a HOM experiment with energy-resolved single electrons injected from mesoscopic capacitor has been performed in the chiral regime<sup>65</sup> and a HOM experiment with time-resolved electrons using the present voltage pulse technique has been performed in the nonchiral regime.<sup>13</sup>

In the following, the HOM shot noise of colliding trains of electron pulses is used as a tool to investigate the time shape of electron wave packets. For simplicity, we will consider, as above, a two-terminal geometry in zero magnetic field. The result can be directly applied to the edge state geometry. Indeed, the noise of a voltage pulse electron source vanishes for unit transmission whatever the pulse shape is. The autocorrelation and cross correlation are thus pure partition noise and have the same amplitude. We consider the periodic injection of charges from both contacts with voltage  $V(t)$  and  $V(t + \tau)$  applied, respectively, on the left and right contacts. The scatterer has transmission  $D$ . In order to compute the shot noise, we use the above photon-assisted Floquet scattering description, with the left and right input operators defined immediately at the left and right entrance of the electronic beam splitter (or scatterer) :

$$\hat{\mathbf{a}}_{L(R)}(\varepsilon) = S(\varepsilon)^{L(R)} \times \hat{\mathbf{a}}_{L(R)}^0(\varepsilon) \quad (21)$$

with

$$S_{l'l'}^{L(R)} = \frac{1}{T} \int_0^T dt \exp[i\phi_{L(R)}(t)] \exp[i2\pi(l - l')\nu t] \quad (22)$$

and  $\phi_L(t) = 2\pi \frac{e}{h} \int_{-\infty}^t V(t') dt'$  and  $\phi_R(t) = 2\pi \frac{e}{h} \int_{-\infty}^{t+\tau} V(t') dt'$ . Then, the shot noise can be calculated as in Sec. II now using both the left and right amplitude probabilities.

Interestingly, in the present case of energy-independent scattering, the gauge invariance property valid at all times, makes the electronic HOM problem *formally equivalent* to the calculation of the shot noise with a single contact, say the left, biased with the voltage difference  $V(t) - V(t + \tau)$  while keeping the right contact at zero. Note the equivalence is only true for a fully coherent system. If not, the reservoir which is a source of decoherence has to be included in the gauge transformation. Consequently, a vanishing HOM shot noise is

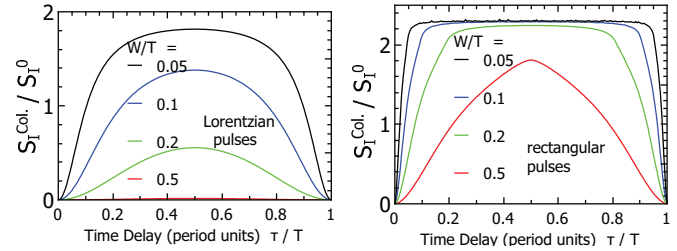


FIG. 15. (Color online) Electron shot noise versus the time delay  $\tau$  for Hong-Ou-Mandel-type correlations for colliding Lorentzian (left) and rectangular (right) pulses. The noise is normalized to  $S_I^0$ .

expected at  $\tau = 0$ , the case of maximal wave-packet overlap or maximal antibunching. However, the fact that the gauge invariance allows us to map the problem to a simpler problem *does not prevent the HOM physics to be the underlying process*. Indeed, we will see below that the HOM noise is directly related to the overlap of the electronic wave functions for periodic trains of wave packets carrying a single electron. A HOM realization not reducible to voltage drop differences via a gauge transformation would, for example, require the use of two single-electron sources based on quantum dots.<sup>65</sup>

Figure 15 gives the calculated shot noise in reduced unit  $S_I^0$  versus the time delay  $\tau/T$  for the collision of single-charge pulses per period emitted by the left and right reservoirs. The left figure corresponds to Lorentzian pulses of different widths and the right figure to discrete Dirac pulses of similar corresponding widths [ $V(t) = h/eW$  if  $0 \leq t \leq W$ ,  $V(t) = 0$  for  $W < t < T$ ]. For both cases, the noise starts from zero at  $\tau = 0$  (perfect antibunching) and is maximum at  $\tau = T/2$  where the wave-packet overlap is minimal. For the Lorentzian case and  $W/T \ll 1$ , the wave packets at  $\tau = T/2$  are well separated and the noise is doubled as two electrons (one from the left, one from the right) contribute independently to single-particle noise at each period. We note, however, that the noise for rectangular pulses exceed the value 2. Indeed, rectangular pulses (which identify to square waves for  $W/T = 0.5$ ) involve a *large amount of neutral excitations* which are measured in the HOM noise.

How far can the HOM noise correlation be used to infer the single-charge wave-packet shape in the time domain? Ideally, one expects the noise to be given by  $2[1 - C(\tau)]$  where

$$C(\tau) = |\langle \Psi(t - \tau - x/v_F) | \Psi(t - x/v_F) \rangle|^2 \quad (23)$$

and  $\Psi$  denotes the wave function of the excess electron injected right above the Fermi sea by the pulse. For Lorentzian pulses, which are clean excitations, a clear positive answer can be given. The shot noise of single-electron colliding Lorentzian pulse is

$$S_I^{\text{Coll}}(\tau)/S_I^0 = \frac{8\beta^2 \sin(\pi\nu\tau)^2}{1 - 2\beta^2 \cos(2\pi\nu\tau) + \beta^4}. \quad (24)$$

The noise is zero for  $\tau = 0$  and for the case of infinite width  $W$  ( $\beta = 0$ ). The maximum noise is  $S_I^0 \frac{2}{\cosh(2\pi W/T)^2}$  for  $\tau = T/2$ .

For  $W/T \rightarrow 0$  (or  $\beta \rightarrow 1$ ), it goes to twice  $S_I^0$  as expected for the partition noise of well-separated single-charge pulses alternatively emitted by the left and right contacts. In this limit, we can use the known expression for the wave function

generated by a single Lorentzian voltage pulse:  $\Psi(t) \propto 1/(t + iW)^2$ . This yields for the square of the wave-function overlap  $C(\tau) = \frac{1}{1+(\tau/2W)^2}$  and this agrees with the limiting expression of Eq. (24):

$$S_I^{\text{Coll}}(\tau)/S_I^0 \simeq 2 \left( 1 - \frac{1}{1+(\tau/2W)^2} \right). \quad (25)$$

In the Appendix, we show that Eq. (24) is also proportional to  $1 - C(\tau)$  even for the case of arbitrary overlap between pulses carrying single electrons. In the small  $W/T$  limit, close expressions have been obtained by Ol'khovskaya *et al.*<sup>23</sup> and by Jonckheere *et al.*<sup>28</sup> (see also Grenier<sup>47</sup>). In these works, single charges whose charge sign periodically alternates are emitted from an ac driven quantum dot capacitor and the trains of charges collide in a QPC. In the adiabatic ac drive limit, the wave packets mimic those emitted by Lorentzian voltage pulses on a contact.

Another striking property of the shot noise of colliding single-charge Lorentzian pulses is the trivial effect of the temperature:  $S_I^{\text{Coll}}(\tau, T_e) = S_I^{\text{Coll}}(\tau, 0)F(T_e)$  where

$$F(T_e) = \frac{1 - \beta^2}{\beta^2} \sum_{l=1}^{\infty} l \beta^{2l} \coth \left( \frac{lh\nu}{2k_B T_e} \right). \quad (26)$$

The time-delay variation and the temperature variation decouple: *thermal fluctuations do not prevent getting accurate information on the time shape of the wave packet*, but they only reduce the noise signal. As shown in the Appendix, this is not true for sine wave pulses and in general for other pulse shapes.

All these remarkable properties demonstrate that, *for integer charge Lorentzian, the HOM shot noise does give information on the time-domain shape of the charge wave packet*. This property is no longer verified for the case of non-Lorentzian pulses as the neutral excitations contribute. The left graph of Fig. 16 shows the value of the HOM noise of Dirac pulses time shifted by  $T/2$  normalized to the partition noise of single pulses, denoted  $S_I^{\text{HBT}}$ . We see that when the overlap between pulses becomes negligible, the ratio tends to twice the single-pulse partition noise. This doubling is expected as now two separate pulses are partitioned per period. For large overlap, the ratio found in Fig. 16 is well smaller than two because of antibunching. An inherent large overlap is also found for a sine wave (right graph of Fig. 16).

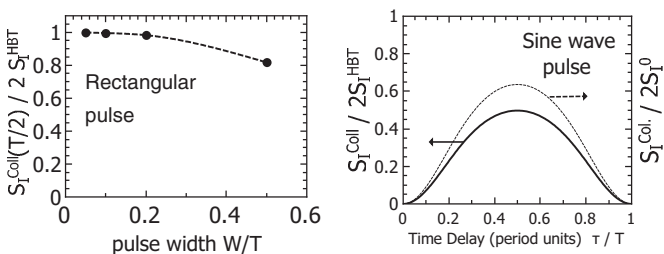


FIG. 16. Left figure: HOM noise at  $\tau = T/2$  for a rectangular pulse normalized to twice the partition noise of a single pulse versus pulse width. Right figure: HOM noise of sine pulses versus  $\tau/T$  normalized to twice the partition noise of single charge (dashed line, right axis) and to twice the single-pulse partition noise (solid line, left axis).

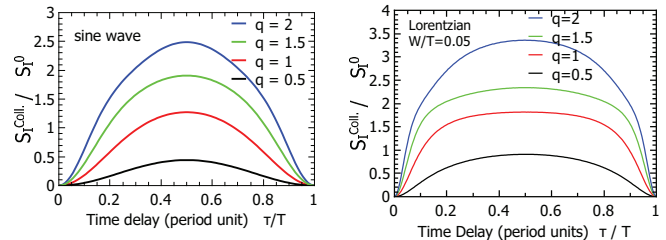


FIG. 17. (Color online) HOM shot noise for sine (left graph) and Lorentzian (right graph) pulses versus time delay and carrying charges  $q = 0.5, 1, 1.5,$  and  $2$ .

Finally, we have calculated the HOM noise of Lorentzian pulses for larger charge, including fractional. For noninteger charge pulses, we do not expect to get simple information on charge pulses in the time domain because of the large content of neutral excitations expected even for the Lorentzian case. The left and right graphs of Fig. 17 show the shot noise for colliding sine wave and Lorentzian pulses for  $q = 0.5, 1, 1.5,$  and  $2$ . For both pulse shapes, the variation with  $\tau$  for  $q = 2$  suggests a double structure related to the interference of several electrons. A detailed study of colliding pulses for large  $q$  will be given elsewhere.<sup>66</sup>

To conclude this section, we have shown that the HOM electronic shot-noise correlation provides meaningful time-domain information on the wave packet. This is true, however, only for a single-charge Lorentzian which is a clean excitation. Other kinds of electron generation are accompanied by a cloud of neutral excitations which contribute to the HOM shot noise and prevent getting time-domain information on the charge part of the excitations.

## VII. CONCLUSION

We have studied in detail the physics of periodic voltage pulses carrying few electrons with the aim to give a useful basis for comparison with experiments.<sup>13</sup> Shot noise, as emphasized in the pioneering papers on Lorentzian voltage pulses, is a tool of choice to characterize the charge pulses. We have exploited the periodicity to show the intimate connection with the well-established physics of photon-assisted shot noise using the powerful Floquet scattering approach. We have used the known properties of PASN as a direct measure of the electron and hole excitation number and, when combined with transport shot noise, as a tool for spectroscopy of the excitations. In the latter case, this provides an energy-domain characterization of the pulses accessible to experiments. This information has been supplemented by a time-domain study of the charge wave packets using HOM-type pulse collisions. The gauge invariance was used to map the charge pulse collision problem to the partitioning of neutral pulses. The comparison of different pulse shapes emphasizes the peculiar nature of Lorentzian pulses with integer charge as ideal electron source. We have also considered pulses with arbitrary charge and show that they always contain a large number of neutral excitations, even for Lorentzian, a manifestation of dynamical orthogonality catastrophe for fermions. For large arbitrary  $q$ , the low-noise property of Lorentzian remains remarkable as the neutral excitation content rapidly decreases with  $q$ , while

it shows a logarithm increases for rectangular shape pulses of the same width, or remains almost constant for sine wave pulses.

Integer charge Lorentzian pulses deliver a noiseless source of few electrons. One expects many applications in quantum physics. For example, by repeating the injection of clean coherent packets with the same electron number and measuring the charge arrived in contacts, the full counting statistics of few electrons partitioned in quantum conductors become accessible. One may also envisage to explore the fermionic statistics of multiple electrons colliding of a beam splitter or interfering in Mach-Zehnder interferometers. Integer charge Lorentzian pulses are also the appropriate source for realizing electronic flying qubits and to entangle few electrons in ballistic conductors. Finally, the powerful approach of Lorentzian pulses could find similar applications in fermionic cold-atom analogs.

### ACKNOWLEDGMENTS

Support from the ERC Advanced Grant No. 228273 MeQuaNo is acknowledged by D.C.G., J.D., T.J., and P.R.. The support from Grant No. ANR-2010-BLANC-0412 is acknowledged by C.G. and P.D.

### APPENDIX

#### 1. Lorentzian voltage pulses carrying arbitrary charge

In this appendix, we calculate the amplitude probabilities  $p_l$  for Lorentzian pulses with arbitrary charges. We start with Eq. (19) with  $n$  replaced by  $q$ :

$$p_l = \int_0^1 du \left( \frac{\sin[\pi(u + i\eta)]}{\sin[\pi(u - i\eta)]} \right)^q \exp[i2\pi(l - q)u]. \quad (A1)$$

Here, the physical decomposition of the voltage into dc and ac parts is essential to avoid ill mathematical behavior. While the Fourier transform of  $\exp[-i\Phi(t)]$  leads to divergent logarithmic terms as  $\Phi(T^-) - \Phi(0^+) = 2\pi q$  is not a multiple of  $2\pi$ , that of the phase associated to the ac part is well defined as  $\phi(T^-) - \phi(0^+) = 0$ .

Defining  $z = \exp(i2\pi u)$  and  $\beta = \exp(-2\pi\eta)$ ,

$$p_l = \frac{\exp(i2\pi q)}{i2\pi} \oint \frac{dz}{z} z^l \left( \frac{1 - \beta z}{1 - \beta \bar{z}} \right)^q. \quad (A2)$$

The numerator has a branch cut singularity for  $z$  on the real axis for  $x > 1/\beta$  and similarly for  $\bar{z}$  in the denominator. Here, we use a series expansion and then perform the integration. Indeed, as  $\beta < 1$  and  $z$  (and  $\bar{z}$ ) are on the unit circle, both the numerator and the denominator are convergent series of positive powers of  $\beta z$  and  $\beta \bar{z}$ , respectively. The integral reduces the double series expansion to a single power series of  $\beta$  by imposing that the power of  $z$  under the integrand is zero. After some algebra, we get

$$p_l = q e^{iq\pi} \beta^l \sum_{k=0}^{\infty} \frac{(-1)^k \beta^{2k} \Gamma(q + l + k)}{\Gamma(k + 1) \Gamma(q - k + 1) \Gamma(l + k + 1)} \quad (A3)$$

for  $l > 0$ , and

$$p_l = q e^{iq\pi} \beta^{|l|} \sum_{p=0}^{\infty} \frac{(-1)^{p+l} \beta^{2p} \Gamma(q + p)}{\Gamma(p + 1) \Gamma(q - |l| - p + 1) \Gamma(|l| + p + 1)} \quad (A4)$$

for  $l < 0$ . Interestingly, while for noninteger  $q$  the sums are infinite (but quickly convergent), for  $q = n$  the sums reduce to the expected polynomial expressions of order  $n - 1$  and the terms for  $l < -n$  vanish. Indeed, when the terms  $(q - k)!$  and  $(q - |l| - p)!$  in the denominator of, respectively, the first and second above expressions are negative integer, they take infinite values which therefore truncate the infinite series.

#### 2. HOM shot-noise calculation

Calculating the HOM noise of colliding electron pulses generated at opposite contacts when applying voltage  $V_L = V(t - \tau/2)$  and  $V_R = V(t + \tau/2)$  on left and right contacts, respectively, is equivalent to calculate the noise when applying  $V(t - \tau/2) - V(t + \tau/2)$  on the left contact only. The resulting zero-temperature shot noise is then

$$S_I/S_I^0 = \sum_{k=-\infty}^{+\infty} |k| |\Pi_k|^2, \quad (A5)$$

where

$$\Pi_k = \frac{1}{T} \int_0^T dt e^{-i\varphi(t-\tau/2)} e^{i\varphi(t+\tau/2)} e^{i2\pi kvt}, \quad (A6)$$

$$\Pi_k = e^{-i2\pi vk\tau/2} \left( \sum_l p_l p_{l-k}^* e^{i2\pi vl\tau} \right), \quad (A7)$$

where  $p_l$  takes the same values as in the main text and is associated to the unshifted potential  $V(t)$ . Because the effective voltage  $V(t - \tau/2) - V(t + \tau/2)$  has symmetric weight for positive and negative values and is symmetric in  $\tau$ , we have  $\Pi_k = e^{-i2\pi kv\tau} \Pi_{-k}^*$ . The shot-noise computation then reduces to calculate

$$S_I/S_I^0 = 2 \sum_{k=1}^{\infty} |k| |\Pi_k|^2. \quad (A8)$$

#### 3. HOM noise of periodic single-charge Lorentzian pulses

To calculate the  $\Pi_k$ , we use the exact values  $p_{(l < -1)} = 0$ ,  $p_{-1} = -\beta$  and  $p_{(l \geq 0)} = (1 - \beta^2)\beta^l$  obtained for single-charge  $q = 1$  Lorentzian voltage pulses. Injecting these values in Eq. (A7), we find

$$\Pi_0 = \frac{1 - (2 - e^{i2\pi v\tau})\beta^2}{1 - \beta^2 e^{i2\pi v\tau}}, \quad (A9)$$

$$\Pi_{l \geq 1} = \beta^l (1 - \beta^2) e^{-i2\pi lv\tau/2} \frac{e^{i2\pi lv\tau} - 1}{1 - \beta^2 e^{i2\pi lv\tau}}. \quad (A10)$$

This allows us to calculate the HOM shot noise for single-charge colliding periodic Lorentzian pulses:

$$S_I^{\text{Coll}}/S_I^0 = \left( 2 \sum_{l=1}^{\infty} l \beta^{2l} \right) \left| \frac{e^{i2\pi v\tau} - 1}{1 - \beta^2 e^{i2\pi v\tau}} \right|^2 (1 - \beta^2)^2, \quad (A11)$$

which gives Eq. (24) of the main text.

To calculate, the temperature dependence one has to replace in Eq. (A10)  $|l|$  by  $l \coth(l\hbar v/2k_B T_e) - 2k_B T_e/\hbar v$ . Interestingly, as  $\Pi_{l \geq 1} = \Pi_1 \beta^{2l}$ , we see that the  $\tau$  dependence is only included in  $\Pi_1$ . The temperature dependence of the HOM shot noise decouples from the  $\tau$  dependence. The temperature only reduces the noise but does not affect the shape.

#### 4. HOM noise of periodic sine wave pulses

Rather than calculating the  $\Pi_l$  using Eq. (A7), it is better to remark that the difference of two sine wave voltages, time shifted by  $\pm\tau/2$ , is also a sine wave. We get  $\Pi_l = J_l[2q \sin(\pi v \tau)]$  for arbitrary charge  $q$  per period. This gives

$$S_I^{\text{Coll}}/S_I^0 = \left( 2 \sum_{l=1}^{\infty} l J_l[2q \sin(\pi v \tau)] \right)^2 \quad (\text{A12})$$

and

$$S_I^{\text{Coll}}/2S_I^{\text{HBT}} = \frac{\sum_{l=1}^{\infty} l J_l[2q \sin(\pi v \tau)]^2}{2 \sum_{l=1}^{\infty} l J_l(q)^2}. \quad (\text{A13})$$

The temperature dependence of the HOM signal can be calculated by replacing  $|l|$  by  $l \coth(l\hbar v/2k_B T_e) - 2k_B T_e/\hbar v$ . We see, however, that the series of Bessel functions in the above expressions does not allow a decoupling of the  $\tau$  and  $T_e$  dependence and the HOM shape is expected to change with temperature. Indeed, the change affects electron and hole pairs with  $l\hbar v \lesssim k_B T_e$  which interact with thermal excitations.

#### 5. Wave-packet interpretation of the Floquet scattering approach

Here, we show that the Floquet approach finds a useful wave-packet interpretation which allows us to calculate the single-electron wave function in the time domain for single-charge pulses. The wave-function overlap can then be computed and be compared with the HOM shot noise. This approach is restricted to zero temperature.

We start with the Martin-Landauer wave packets<sup>41</sup> defined in the energy bandwidth  $\hbar v$ . Without loss of generality, the wave functions describing the states of the, say left, reservoir  $\sim e^{-i\varepsilon(t-x/v_F)/\hbar}$  and labeled by the continuous energy variable  $\varepsilon$  can be transformed into a set of orthogonal wave packets  $\varphi_{n,l}(t-x/v_F)$  defined by integration over the energy window  $\varepsilon \in [l\hbar v, (l+1)\hbar v]$ . Defining  $u = (t-x/v_F)/T$ ,

$$\varphi_{n,l}(t-x/v_F) = \frac{1}{\sqrt{2\pi\hbar V_F}} \frac{\sin[\pi(u-n)]}{\pi(u-n)} e^{-i2\pi v(l+1/2)(u-n)}. \quad (\text{A14})$$

Using the annihilation operators  $\hat{a}_{n,l}^0$  acting on the Fock states of the unperturbed reservoir, the fermion operator before the action of the ac potential is

$$\hat{\Psi}^0(t-x/v_F) = \sum_l \sum_n \varphi_{n,l}(t-x/v_F) \hat{a}_{n,l}^0 \quad (\text{A15})$$

with  $\langle \hat{a}_{n',l'}^0 \hat{a}_{n,l}^0 \rangle = \delta_{n,n'} \delta_{l,l'} f_l$  and  $f_l = 1$  for  $l < 0$  and  $f_l = 0$  for  $l \geq 0$ . After the electrons have experienced the potential

$V(t)$ , the electron fermion operator becomes

$$\hat{\Psi}(t-x/v_F) = \sum_k \sum_l \sum_n p_k \varphi_{n,l}(t-x/v_F) \hat{a}_{n,l-k}^0. \quad (\text{A16})$$

We see that the ac potential does not mix wave packets of different  $n$  but only wave packets of different energies and same  $n$  [we can also see that  $\sum_l p_l \varphi_{n,l}(t-x/v_F)$  forms a new orthogonal basis of wave functions].

#### 6. Hong-Ou-Mandel correlation for single-charge Lorentzian periodic pulses

We remind that the HOM noise associated with independent Lorentzian voltage pulses carrying one electron is directly related to the overlap of the electron wave function in the beam splitter. Here, we would like to see if a generalization is possible in the case of a periodic train of overlapping Lorentzian pulses still carrying only one electron. To do that, instead of the wave-function overlap we consider the time-average Hermitian product of the electron fermion operators with a relative time shift  $\tau$ . Using the reduced variable  $\theta = \tau/T$  it is given, before time averaging, by

$$\begin{aligned} & \left\langle \hat{\Psi}^\dagger \left( u + \frac{\theta}{2} \right) \hat{\Psi} \left( u - \frac{\theta}{2} \right) \right\rangle \\ &= \sum_{l'l'} \sum_{nn'} \sum_{kk'} p_{k'}^* p_k \varphi_{n',l'+k'}^* \left( u + \frac{\theta}{2} \right) \\ & \quad \times \varphi_{n,l+k} \left( u - \frac{\theta}{2} \right) \langle \hat{a}_{n',l'}^0 \hat{a}_{n,l}^0 \rangle. \end{aligned} \quad (\text{A17})$$

After time averaging and subtracting the contribution of the Fermi sea [i.e., with no  $V(t)$ ], we get

$$\overline{\left\langle \hat{\Psi}^\dagger \left( u + \frac{\theta}{2} \right) \hat{\Psi} \left( u - \frac{\theta}{2} \right) \right\rangle} = \left( \frac{\sin(\pi\theta)}{\pi\theta} \right)^2 C(\tau), \quad (\text{A18})$$

where

$$C(\tau) = \left| \sum_l f_l e^{i2\pi l\theta} \sum_k (P_k - \delta_{k,0}) e^{i2\pi k\theta} \right|^2. \quad (\text{A19})$$

For the presently considered case of periodic Lorentzian voltage pulses carrying unit charge and using the probabilities defined with respect to the total voltage  $V(t) = V_{\text{dc}} + V_{\text{ac}}(t)$ , i.e.,  $P_0 - 1 = \beta^2 - 1$  and  $P_l = (1 - \beta^2)^2 \beta^{2(l-1)}$  for  $l \geq 1$ , we get

$$C(\tau) = \frac{(1 - \beta^2)^2}{1 - 2\beta^2 \cos(2\pi\tau/T) + \beta^4}. \quad (\text{A20})$$

It is then straightforward to show that  $1 - C(\tau)$  yields the HOM shot noise given by Eq. (24), i.e.,

$$S_I^{\text{HOM}} = 2S_I^0 [1 - C(\tau)]. \quad (\text{A21})$$

Thus, even for overlapping pulses (but carrying a single electron), the HOM noise can still be interpreted as a measure of the overlap of the electronic wave function.

- <sup>1</sup>L. S. Levitov, H. Lee, and G. Lesovik, *J. Math. Phys.* **37**, 4845 (1996); D. A. Ivanov, H. W. Lee, and L. S. Levitov, *Phys. Rev. B* **56**, 6839 (1997).
- <sup>2</sup>J. Keeling, I. Klich, and L. S. Levitov, *Phys. Rev. Lett.* **97**, 116403 (2006).
- <sup>3</sup>L. S. Levitov and G. B. Lesovik, *Pis'ma v ZhETF*, **58**(3), 225 (1993) [*JETP Lett.* **58**, 230 (1993)].
- <sup>4</sup>See, for example, F. Hassler, M. V. Suslov, G. M. Graf, M. V. Lebedev, G. B. Lesovik, and G. Blatter, *Phys. Rev. B* **78**, 165330 (2008).
- <sup>5</sup>A. Bertoni, P. Bordone, R. Brunetti, C. Jacoboni, and S. Reggiani, *Phys. Rev. Lett.* **84**, 5912 (2000).
- <sup>6</sup>R. Ionicioiu, G. Amaratunga, and F. Udrea, *Int. J. Mod. Phys.* **15**, 125 (2001).
- <sup>7</sup>T. M. Stace, C. H. W. Barnes, and G. J. Milburn, *Phys. Rev. Lett.* **93**, 126804 (2004).
- <sup>8</sup>Michael Moskalets and Markus Büttiker, *Phys. Rev. B* **83**, 035316 (2011).
- <sup>9</sup>F. Hassler, G. B. Lesovik, and G. Blatter, *Phys. Rev. Lett.* **99**, 076804 (2007).
- <sup>10</sup>M. Vanevic, Y. V. Nazarov, and W. Belzig, *Phys. Rev. B* **78**, 245308 (2008).
- <sup>11</sup>A. V. Lebedev and G. Blatter, *Phys. Rev. Lett.* **107**, 076803 (2011).
- <sup>12</sup>G. Haack, H. Förster, and M. Büttiker, *Phys. Rev. B* **82**, 155303 (2010).
- <sup>13</sup>J. Dubois, T. Jullien, P. Roulleau, F. Portier, P. Roche, Y. Jin, A. Cavanna, W. Wegscheider, and D. C. Glattli (unpublished).
- <sup>14</sup>L. J. Geerligs, V. F. Anderegg, P. A. M. Holweg, J. E. Mooij, H. Pothier, D. Estève, C. Urbina, and M. H. Devoret, *Phys. Rev. Lett.* **64**, 2691 (1990).
- <sup>15</sup>H. Pothier, P. Lafarge, C. Urbina, and M. H. Devoret, *Europhys. Lett.* **17**, 249 (1992).
- <sup>16</sup>J. M. Shilton, V. I. Talyanskii, M. Pepper, D. A. Ritchie, J. E. F. Frost, C. J. B. Ford, C. G. Smith, and G. A. C. Jones, *J. Phys.: Condens. Matter* **8**, L531 (1996); V. I. Talyanskii, J. M. Shilton, M. Pepper, C. G. Smith, C. J. B. Ford, E. H. Linfield, D. A. Ritchie, and G. A. C. Jones, *Phys. Rev. B* **56**, 15180 (1997).
- <sup>17</sup>S. Hermelin, S. Takada, M. Yamamoto, S. Tarucha, A. D. Wieck, L. Saminadayar, C. Bäuerle and T. Meunier, *Nature (London)* **477**, 435 (2011).
- <sup>18</sup>R. P. G. McNeil, M. Kataoka, C. J. B. Ford, C. H. W. Barnes, D. Anderson, G. A. C. Jones, I. Farrer, and D. A. Ritchie, *Nature (London)* **477**, 439 (2011).
- <sup>19</sup>J. Gabelli, G. Fève, J.-M. Berroir, B. Plaçais, A. Cavanna, B. Etienne, Y. Jin, and D. C. Glattli, *Science* **313**, 499 (2006).
- <sup>20</sup>G. Fève, A. Mahé, J.-M. Berroir, T. Kontos, B. Plaçais, D. C. Glattli, A. Cavanna, B. Etienne, and Y. Jin, *Science* **316**, 1169 (2007).
- <sup>21</sup>E. Bocquillon, F. D. Parmentier, C. Grenier, J.-M. Berroir, P. Degiovanni, D. C. Glattli, B. Plaçais, A. Cavanna, Y. Jin, and G. Fève, *Phys. Rev. Lett.* **108**, 196803 (2012).
- <sup>22</sup>J. Splettstoesser, S. Ol'khovskaya, M. Moskalets, and M. Büttiker, *Phys. Rev. B* **78**, 205110 (2008).
- <sup>23</sup>S. Olkhovskaya, J. Splettstoesser, M. Moskalets, and M. Büttiker, *Phys. Rev. Lett.* **101**, 166802 (2008).
- <sup>24</sup>Janine Splettstoesser, Michael Moskalets, and Markus Büttiker, *Phys. Rev. Lett.* **103**, 076804 (2009).
- <sup>25</sup>Geraldine Haack, Michael Moskalets, Janine Splettstoesser, and Markus Büttiker, *Phys. Rev. B* **84**, 081303 (2011).
- <sup>26</sup>Mathias Albert, Christian Flindt, and Markus Büttiker, *Phys. Rev. Lett.* **107**, 086805 (2011).
- <sup>27</sup>Y. Sherkunov, N. d'Ambrumenil, P. Samuelsson, and M. Büttiker, *Phys. Rev. B* **85**, 081108 (2012).
- <sup>28</sup>T. Jonckheere, J. Rech, C. Wahl, and T. Martin, *Phys. Rev. B* **86**, 125425 (2012).
- <sup>29</sup>G. B. Lesovik and L. S. Levitov, *Phys. Rev. Lett.* **72**, 538 (1994).
- <sup>30</sup>M. H. Pedersen and M. Büttiker, *Phys. Rev. B* **58**, 12993 (1998).
- <sup>31</sup>V. S. Rychkov, M. L. Polianski, and M. Büttiker, *Phys. Rev. B* **72**, 155326 (2005).
- <sup>32</sup>M. Vanevic, Y. V. Nazarov, and W. Belzig, *Phys. Rev. Lett.* **99**, 076601 (2007).
- <sup>33</sup>D. Bagrets and F. Pistolesi, *Phys. Rev. B* **75**, 165315 (2007).
- <sup>34</sup>M. Moskalets and M. Büttiker, *Phys. Rev. B* **66**, 205320 (2002).
- <sup>35</sup>R. J. Schoelkopf, A. A. Kozhevnikov, D. E. Prober, and M. J. Rooks, *Phys. Rev. Lett.* **80**, 2437 (1998).
- <sup>36</sup>L.-H. Reydellet, P. Roche, D. C. Glattli, B. Etienne, and Y. Jin, *Phys. Rev. Lett.* **90**, 176803 (2003).
- <sup>37</sup>G. B. Lesovik, *Pis'ma Zh. Eksp. Teor. Fiz.* **49**, 513 (1989) [*JETP Lett.* **49**, 592 (1989)].
- <sup>38</sup>V. A. Khlus, *Zh. Eksp. Teor. Fiz.* **93**, 2179 (1987) [*Sov. Phys.-JETP* **66**, 1243 (1987)].
- <sup>39</sup>B. Yurke and G. P. Kochanski, *Phys. Rev. B* **41**, 8184 (1990).
- <sup>40</sup>M. Büttiker, *Phys. Rev. Lett.* **65**, 2901 (1990); *Phys. Rev. B* **46**, 12485 (1992).
- <sup>41</sup>Th. Martin and R. Landauer, *Phys. Rev. B* **45**, 1742 (1992).
- <sup>42</sup>Y. M. Blanter and M. Büttiker, *Phys. Rep.* **336**, 1 (2000).
- <sup>43</sup>M. Reznikov, M. Heiblum, H. Shtrikman, and D. Mahalu, *Phys. Rev. Lett.* **75**, 3340 (1995).
- <sup>44</sup>A. Kumar, L. Saminadayar, D. C. Glattli, Y. Jin, and B. Etienne, *Phys. Rev. Lett.* **76**, 2778 (1996).
- <sup>45</sup>H. W. Lee and L. S. Levitov, [arXiv:cond-mat/9312013](https://arxiv.org/abs/cond-mat/9312013).
- <sup>46</sup>P. W. Anderson, *Phys. Rev. Lett.* **18**, 1049 (1967).
- <sup>47</sup>C. Grenier, R. Hervé, E. Bocquillon, F. D. Parmentier, B. Plaçais, J. M. Berroir, G. Fève, and P. Degiovanni, *New J. Phys.* **13**, 093007 (2011).
- <sup>48</sup>M. Büttiker, A. Prêtre, and H. Thomas, *Phys. Rev. Lett.* **70**, 4114 (1993).
- <sup>49</sup>C. Grenier, J. Dubois, T. Jullien, P. Roulleau, D. C. Glattli, and P. Degiovanni, *Phys. Rev. B* **88**, 085302 (2013).
- <sup>50</sup>M. Moskalets and M. Büttiker, *Phys. Rev. B* **73**, 125315 (2006).
- <sup>51</sup>H. W. Lee and L. S. Levitov, [arXiv:cond-mat/9507011](https://arxiv.org/abs/cond-mat/9507011).
- <sup>52</sup>A. A. Kozhevnikov, Ph.D. thesis, Yale University, 2001, <http://www.yale.edu/proberlab/Papers/alexthesis.pdf>.
- <sup>53</sup>A. V. Shytov, *Phys. Rev. B* **71**, 085301 (2005).
- <sup>54</sup>J. Torrès, T. Martin, and G. B. Lesovik, *Phys. Rev. B* **63**, 134517 (2001).
- <sup>55</sup>A. Crépieux, P. Devillard, and T. Martin, *Phys. Rev. B* **69**, 205302 (2004).
- <sup>56</sup>D. Chevallier, T. Jonckheere, E. Paladino, G. Falci, and T. Martin, *Phys. Rev. B* **81**, 205411 (2010).
- <sup>57</sup>In the different context of the periodic injection of energy-resolved electron and holes above the Fermi sea from a mesoscopic capacitor, the noise of electron and hole partitioned by a QPC was found reduced by thermal excitations in Ref. 21 and its origin discussed and compared with experiments.
- <sup>58</sup>J. Gabelli and B. Reulet, *Phys. Rev. B* **87**, 075403 (2013).
- <sup>59</sup>T. Jonckheere, M. Creux, and T. Martin, *Phys. Rev. B* **72**, 205321 (2005).
- <sup>60</sup>C. K. Hong, Z. Y. Ou, and L. Mandel, *Phys. Rev. Lett.* **59**, 2044 (1987).

- <sup>61</sup>H. Fearn and R. Loudon, *J. Opt. Soc. Am. B* **6**, 917 (1989).
- <sup>62</sup>R. Loudon, *Phys. Rev. A* **58**, 4904 (1998).
- <sup>63</sup>V. Giovannetti, D. Frustaglia, F. Taddei, and R. Fazio, *Phys. Rev. B* **74**, 115315 (2006).
- <sup>64</sup>A. V. Lebedev and G. Blatter, *Phys. Rev. B* **77**, 035301 (2008).
- <sup>65</sup>E. Bocquillon, V. Freulon, J.-M. Berroir, P. Degiovanni, B. Plaçais, A. Cavanna, Y. Jin, and G. Feve, *Science* **339**, 1054 (2013).
- <sup>66</sup>D. C. Glatli (unpublished).
- <sup>67</sup>M. D. Blumenthal, B. Kaestner, L. Li, S. Giblin, T. J. B. M. Janssen, M. Pepper, D. Anderson, G. Jones, and D. A. Ritchie, *Nat. Phys.* **3**, 343 (2007).